



HAL
open science

Transmembrane chemical absorption technology for ammonia recovery from wastewater: A critical review

Irene Gonzalez-Salgado, Christelle Guigui, Mathieu Sperandio

► To cite this version:

Irene Gonzalez-Salgado, Christelle Guigui, Mathieu Sperandio. Transmembrane chemical absorption technology for ammonia recovery from wastewater: A critical review. *Chemical Engineering Journal*, 2022, 444, 10.1016/j.cej.2022.136491 . hal-03699160

HAL Id: hal-03699160

<https://hal.inrae.fr/hal-03699160v1>

Submitted on 22 Jul 2024

HAL is a multi-disciplinary open access archive for the deposit and dissemination of scientific research documents, whether they are published or not. The documents may come from teaching and research institutions in France or abroad, or from public or private research centers.

L'archive ouverte pluridisciplinaire **HAL**, est destinée au dépôt et à la diffusion de documents scientifiques de niveau recherche, publiés ou non, émanant des établissements d'enseignement et de recherche français ou étrangers, des laboratoires publics ou privés.



Distributed under a Creative Commons Attribution - NonCommercial 4.0 International License

Transmembrane chemical absorption technology for ammonia recovery from wastewater: a critical review

Irene Gonzalez Salgado^a, Christelle Guigui^a, Mathieu Sperandio^a

^aTBI, Université de Toulouse, CNRS, INRAE, INSA, Toulouse, France (e-mail : sperandio@insa-toulouse.fr)

Transmembrane chemical absorption technology for ammonia recovery from wastewater: a critical review

Abstract

Technologies for resource recovery from wastewater have drawn the world's attention. Recovering nitrogen contained in wastewater offers an opportunity to produce alternative fertilizers for agriculture instead of conventional treatment. Transmembrane chemical absorption is a promising process based on hydrophobic membrane contactors to recover ammonia from wastewater to produce an ammonium-based product. This review critically explores the process principle, modelling approaches, membrane materials and system configurations, mass transfer characterization, elucidation of the undesired phenomenon of water vapour transport and a particular focus on influencing operating conditions. Ammonia could be recovered from a wide range of waste, including digestate, urine, manure or industrial effluents. The pretreatment of the wastewater, as well as membrane fouling and wetting, are identified as major challenges facing this technology. Operating experience with full and pilot-scale plants is analyzed to assess present and future research questions regarding this emerging technology.

Keywords: ammonia recovery, hydrophobic membrane, wastewater, nutrient recovery, fertilizer

Table of content

Abstract	2
Table of content.....	3
1. Introduction.....	5
2. Principle and theoretical concept	6
3. Membrane typologies and process classification.....	10
4. Process configuration, mass balance and mass transfer coefficients determination.....	12
4.1. System a: External membrane contactor without feed recirculation.....	12
4.2. System b: External membrane contactor with feed recirculation.....	14
4.3. System c: Membrane contactor submerged in the feed solution.....	15
4.4. Modelling studies for predicting transfer coefficients of TMCS	17
5. Influencing parameters and optimal design	19
5.1. pH and temperature	19
5.2. Effect of feed stream liquid velocity	21
5.3. Influence of initial ammonia concentration.....	21
5.4. Effect of salinity on feed solution.....	22
5.5. Stripping solution: nature, concentration and liquid velocity.....	23
6. Limiting factors.....	25

6.1. Water vapour transport	25
6.2. Impact of suspended solids and fouling phenomenon.....	27
7. Practical feedbacks and future needs for a scale-up	28
8. Acknowledgements.....	33
9. References.....	34
10. Tables and figures	41

1. Introduction

Wastewater is progressively considered a resource of water and nutrients to face water scarcity and the perturbation of nutrient cycles by human activities. A paradigm shift in wastewater handling and treatment system design is encouraged. While treatment technologies are continuously advancing to address new challenges, wastewater treatment plants are likely to be transformed into resource recovery facilities [1]. Whereas technologies for phosphorus recovery are progressively implemented on sludge streams, very few applications are still visible for nitrogen recovery. It is, however, demonstrated that nitrogen recovery is one of the most critical challenges for the future to make wastewater management less environmentally impacting and provide a sustainable solution for future proteins production [2].

The technology of TMCS gained significant attention among other membrane-based processes applied for nutrient recovery. The term TMCS was initially used for TransMembraneChemiSorption, but it should be mentioned that there is no chemisorption mechanism in this process. It should be more accurately defined as TransMembrane Chemical abSorption [3]. TMCS is also known as membrane stripping [4], supported gas membrane (SGM) [5], gas permeable hydrophobic membrane [6], gas-membrane absorption (GMA) [7] or use of a hollow-fibre membrane contactor for ammonia recovery. This process is particularly interesting since hydrophobic membranes allow the specific transfer of ammonia from waste streams and recovery in a valuable ammonium salt fertilizer. TMCS offers several advantages such as a high transfer surface area, relatively low pressure compared to other membrane applications and negligible contamination in the recovered product [8,9].

Researchers reviewed recent advancements in processes developed for nutrient recovery from waste streams [10–12], from digestate [13] and human excreta for subsequent

agricultural applications [14,15]. Hou et al., (2019) [16] provided a critical review about hydrophobic membranes applied to gas extraction, delivery and hybrid processes from wastewater. More specifically about ammonia recovery, critical reviews were focused on the treatment of side-streams of WWTPs [17], manure [18] or membrane-based processes [19]. Darestani et al., (2017) [20] reviewed specifically the current status of hollow-fibre membrane contactors and highlighted its specific application for ammonia recovery from wastewater. It was recommended to focus upon a greater understanding of the process engineering involved. Despite all the promising results, there is still a lack of critical review concerning the different configurations and applications of TMCS, as well as the impact of influencing parameters and modelling studies.

In this context, the following review aims to present recent advances in transmembrane chemisorption technology from waste streams, highlight state-of-the-art successful applications and modelling studies. In particular, the effect of operating conditions on transfer efficiency, a critical elucidation and homogenization of mass transfer characterization, recommendations for process scale-up and research perspectives for the TMCS process are addressed.

2. Principle and theoretical concept

TMCS is a membrane-based process that allows transferring ammonia from an aqueous stream to another through a hydrophobic membrane.

Total ammonia nitrogen (TAN) refers to the sum, in an aqueous solution, of free ammonia NH_3 and ionized form ammonium, NH_4^+ , whose ratio is controlled by dissociation equilibrium (1):

$$K_a = \frac{[NH_3] \cdot [H^+]}{[NH_4^+]} \quad (1)$$

where K_a is the acid dissociation constant for ammonia equilibrium.”

Two-film theory can be applied in the case of a porous membrane if membrane resistance is considered [21]. In TMCS, the dissolved ammonia ($NH_{3(aq)}$) diffuses across a first boundary layer (δ_L) from the feed bulk to the liquid-gas interface at the pore entrance. Then, $NH_{3(aq)}$ volatilizes at the liquid-gas interface and ammonia gas ($NH_{3(g)}$) diffuses into the air-filled pores of the hydrophobic membrane. Finally, $NH_{3(g)}$ is dissolved into the acid solution in which it reacts instantaneously with the protons of the solution on the gas-liquid interface (Figure 1). In the two-film theory, equilibrium at the gas-liquid interface is assumed, and partial pressure (P_{NH_3}) and concentration (C_{NH_3}) at the interface can be calculated with Henry’s law. Nitric and phosphoric acids [9,22–24] can be used as a stripping solution, but sulfuric acid is the most commonly used, producing ammonium sulphate (2), a well-established fertilizer.



The mass transfer can be expressed by considering a resistance-in-series model [5,25–28]. The overall mass transfer coefficient (K_{ov}) can be calculated as the sum of individual coefficients in a three-resistance model: (i) liquid film on shell side ($1/k_s$), (ii) membrane resistance ($1/k_m$) and (iii) lumen side ($1/k_l$).

$$\frac{1}{K_{ov}} = \frac{1}{k_s} + \frac{1}{k_m} + \frac{1}{k_l} \quad (3)$$

Resistance at the acid side (k_l) is generally considered negligible because ammonia is protonated in contact with the acid side and reacts extremely rapidly with the acid in the boundary layer at the membrane surface [5,28]. The rate constant of chemical reaction (2) is

several magnitudes greater than the mass transfer coefficient [29], then the process will be controlled by the ammonia diffusion in the feed stream and membrane pores.

For assessing the performance of the TMCS process, it is common to consider that the overall mass transfer coefficient is mainly influenced by the resistance on the liquid side of the feed solution and membrane resistance.

The driving force of the mass transfer in the TMCS process is the gradient of ammonia partial pressure between feed and stripping streams [24,28,30–34] as a result of the concentration difference across the membrane. A key parameter for an efficient ammonia transfer is the maximization of free ammonia fraction that can be promoted via appropriate pH and temperature control. Vecino et al., (2019) [24] defined the ammonia flux (J_{NH_3} , $Kmol\ m^{-2}\ s^{-1}$) as expression (4).

$$J_{NH_3} = \frac{K_{ov} \cdot (p_{NH_3}^{bulk\ feed} - p_{NH_3}^{stripping\ solution})}{R \cdot T} \quad (4)$$

Where K_{ov} ($m\ s^{-1}$) the overall mass transfer coefficient that combines all the theoretical resistances (3); $p_{NH_3}^{bulk\ feed}$ (atm) and $p_{NH_3}^{stripping\ solution}$ (atm) are the ammonia partial pressures of the feed and stripping solution; T (K) is the temperature and R ($atm\ m^3\ Kmol^{-1}\ K^{-1}$) the ideal gas constant. The ammonia flux (J_A) is frequently expressed with the following simplified expression, considering the ideal gas law ($P_A = C_A \cdot R \cdot T$).

$$J_A = K_{ov} \cdot (C_A^{bulk\ feed} - C_A^*) \quad (5)$$

Where K_{ov} the overall mass transfer coefficient that combines all the theoretical resistances (3); $C_A^{bulk\ feed}$ the ammonia concentration in the bulk feed solution and C_A^* the ammonia concentration at the gas-liquid interface (acid side) that would be in equilibrium with the

dissolved ammonia in the bulk acid, which will be equal to zero because ammonia is instantaneously protonated in contact to the acid stream at low pH ($p_{NH_3}^{stripping\ solution} \ll p_{NH_3}^{bulk\ feed}$). This is a valid assumption when acid is in excess to ensure the reaction. The increase of membrane area increases the ammonia transfer rate as it can be inferred from equation (5).

In general, the mass transfer coefficient, K_{TAN} (6), can be determined based on total ammonia/ammonium concentration when TAN concentrations are considered [5,35–40]. K_{FA} (7), if free ammonia fraction (FA) is considered [38,41,42,30,43–45]. Less frequently, K_{FAG} (8) can be calculated based on free ammonia gas ($NH_3-N_{(g)}$) also considering Henry's constant (H) [46].

$$J_{TAN} = K_{TAN} \cdot (C_{TAN}^{bulk\ feed} - C_{TAN}^*) \quad (6)$$

$$J_{FA} = K_{FA} \cdot FA \cdot (C_{NH_3-N(aq)}^{bulk\ feed} - C_{NH_3-N(aq)}^*) \quad (7)$$

$$J_{FAG} = K_{FAG} \cdot FA \cdot H \cdot (C_{NH_3-N(g)}^{bulk\ feed} - C_{NH_3-N(g)}^*) \quad (8)$$

These equations simplify the driving force of mass transfer to the concentration difference at the liquid-gas interface and the bulk solution. However, this difference is not considered constant along membrane contactor for ammonia concentrated solutions. Alternatively, the logarithmic mean concentration difference, ΔC_{lm} (9), can represent an average concentration by considering the ammonia concentration at the inlet and outlet of the contactor.

$$\Delta C_{LM} = \left(\frac{(C_{TAN,feed\ in} - C_{TAN,feed\ in}^*) - (C_{TAN,feed\ out} - C_{TAN,feed\ out}^*)}{\ln\left(\frac{C_{TAN,feed\ in} - C_{TAN,feed\ in}^*}{C_{TAN,feed\ out} - C_{TAN,feed\ out}^*}\right)} \right) \quad (9)$$

As explained before, C_i^* is equal to 0, substituting in equation (9) the logarithmic mean difference will be the same for the case of counter or co-current flow.

3. Membrane typologies and process classification

Depending on the objective of the application, several configurations for membrane contactors are possible, alternating between pressurized membrane vessels [40], submerged membrane modules [30,47], using multiple membrane modules connected in series [48,49] or even placed in the headspace in order to recovery free ammonia gas from the air [46,50]. While most of the current TMCS studies focused on lab-scale applications, only three full-scale plants have been operating [49,51,52]. The membrane module provided by Membrana GmbH-3M company is the most widely extended (Figure S.1).

In Table 1, we proposed a classification of the different TMCS membrane technologies based on material, geometry and stream flows. Hydrophobic membranes used in TMCS are mainly made of polypropylene (PP), polytetrafluoroethylene (PTFE), expanded polytetrafluoroethylene (e-PTFE) and polyvinylidene fluoride (PVDF). Poly(4methyl-1-pentene) (PMP) has recently been study for ammonia removal application. PTFE is the most common material for hydrophobic membrane applications because of its high thermal stability and chemical resistance compared to PVDF and PP, which is less expensive [16]. Two laboratory-scale studies indicated that PTFE could have better behaviour against fouling than PP [53,54] (see 6.2). The first use of PMP material showed promising results [34], obtaining similar ammonia recovery efficiency compared to other cited materials. However, little

information is found comparing the performance of mentioned materials in TMCS facility with similar geometry and operating condition.

Three types of membrane geometries were used: hollow-fibre, flat-sheet and tubular membrane. Feed and stripping streams were circulated in co-current or countercurrent, on lumen or shell side for tubular membrane and hollow-fibre, with or without recirculation. Feed or stripping solution can be stored in a vessel while the other stream is pumped through the membrane. Combining these criteria, twelve different configurations were distinguished (Table 1).

The most common reported set-ups concerning streams arrangement in the membrane module are: (i) feed flows in lumen side, and stripping solution in shell side; (ii) feed flows in shell side, and stripping solution in lumen side; (iii) fibres are submerged in a vessel containing the feed solution, and stripping solution flows inside the fibres. Most authors agreed on the acid recirculation and the addition of concentrated acid to ensure the transfer and reaction, obtaining a concentrated solution of an ammonium salt [24,42,46,49,55].

The influence of the placement of the feed and stripping solutions is little studied. When options (i) and (ii) were compared, Hasanoğlu et al., (2010) [25] found higher ammonia removal when the feed stream was flowing in the shell side and the stripping stream in the lumen side. In the case of disposition (iii), Wäeger-Baumann et Fuchs, (2012) [38] compared the impact on the mass transfer coefficient when anaerobic digestate (feed solution) was flowing in lumen side and sulfuric acid (stripping solution) was stored in the vessel, and inversely. They obtained a coefficient 1.5 times higher when feed solution was flowing in the lumen side, but an additional step of ultrafiltration was necessary as pretreatment to avoid solid pore blocking of the hollow fibres. Up to now, this study was the only one of the options (iii) and feed stream flowing inside the fibres.

There is no general choice of the polymer and configuration. The selection will depend on the type of feed and process. First pilot-scale treating digestate adopted configuration 1 (Table 1), where feed is recirculated inside the fibres of a hollow-fibre contactor after an ultrafiltration step. However, all full-scale applications treating digestate have chosen configuration 5 (Table 1) with a PP hollow-fibre module and stripping solution recirculation, reducing the filtration step necessary to flow inside the fibres. In addition, the feed could be treated in a single pass if enough membrane surface is provided. Otherwise, several pilot-scales facilities have adopted configuration 9 (Table 1), where membrane contactors are directly submerged in the feed tank. This system could avoid all the pretreatment steps of the feed. However, the ammonia recovery efficiency reported was lower, maybe because the difficulty to adapt the feed conditions to the pH and temperature required to maximize NH_3 form. This configuration can present a significant interest for ammonia mitigation in livestock operations.

4. Process configuration, mass balance and mass transfer coefficients determination

4.1. System a: External membrane contactor without feed recirculation

For a set-up where feed flows in an open-loop system (Figure 2a), the overall mass transfer coefficient is determined based on a mass balance (10) in the feed flow along the membrane module [56]. This balance can be applied to configurations 3, 5 and 12 (Table 1). It is also assumed that the acid concentration is always in excess to ensure the ammonia reaction (2) without the influence of the acid recirculation.

$$-Q dC_{TAN} = K_{TAN} (C_{TAN,feed} - C_{TAN, feed}^*) dA_M \quad (10)$$

Where Q stands for the flow rate of the feed stream; A_M is the membrane surface (interfacial area of mass exchange); $C_{TAN, feed}$ is the concentration of ammonia in the membrane contactor, $C_{N-NH_3, feed}^*$ is the ammonia concentration at the gas-liquid interface (acid side) that would be zero (see 2).

The integration and linearization of expression (10) with the substitution of boundary limits of the differential area, A varies between 0 and A_M and concentrations between $C_{TAN, feed in}$ and $C_{TAN, feed out}$, allow to obtain the overall mass transfer coefficient K_{TAN} .

$$\ln\left(\frac{C_{TAN, feed in}}{C_{TAN, feed out}}\right) = K_{TAN} \frac{A_M}{Q} \quad (11)$$

Where $C_{TAN, feed in}$ and $C_{TAN, feed out}$ are the ammonia concentrations of the feed before and after their passage through the membrane contactor, respectively (Figure 2a).

A_M can be expressed when feed flows inside the fibres in terms of the inner diameter of the hollow fibre (D_i), number of fibres (N_f) and fibre length (L):

$$A_M = N_f \pi D_i L \quad (12)$$

And the flow rate as a function of cross-sectional area ($S = \pi D_i^2/4$) and the speed of the feed in the section (v):

$$Q = N_f S v \quad (13)$$

Combining equations (11), (12), (13) and a , the interfacial area per unit volume of the fibre $4/D_i$, equation (11) is expressed as:

$$\ln\left(\frac{C_{TAN, feed in}}{C_{TAN, feed out}}\right) = K_{TAN} \frac{a L}{v} \quad (14)$$

When feed flows in the shell-side, D_i can be replaced for the hydraulic diameter (D_h). In the case of a cross-flow hollow fibre membrane module (Figure S.1), D_h is calculated by equation (15):

$$D_h = \frac{d_m^2 - d_t^2 - N_f D_i^2}{N_f D_i} \quad (15)$$

Where d_m is the inside diameter of the cartridge and d_t is the outside diameter of the centre feed.

4.2. System b: External membrane contactor with feed recirculation

In this set-up, feed is recirculated in a tank. We assumed uniform mixing in the tank and acid concentration always in excess to ensure the ammonia reaction (2), then the recirculation of the acid stream does not influence the mass transfer, and the co/countercurrent flows either.

The mass balance on the feed tank is written as expression (16):

$$V \frac{d}{dt} C_{TAN,tank} = Q (C_{TAN,feed\ out} - C_{TAN,tank}) \quad (16)$$

Where $C_{TAN, tank}$ is the concentration of ammonia in the tank.

After integrating mass balance (16) with the substitution of boundary limits of time and concentration ($t=0$, $C_{TAN, tank} = C_{TAN, tank, t0}$; $t=t$, $C_{TAN, tank} = C_{TAN, tank, t}$) and replacing $C_{TAN, feed\ out}$ from equation (14) we obtain:

$$\ln \left(\frac{C_{TAN,tank, t0}}{C_{TAN,tank, t}} \right) = \frac{Q}{V} \left(1 - e^{-\frac{K_{TAN} a L}{v}} \right) \cdot t \quad (17)$$

This balance was reported in configurations 1, 7, 11 and 12 (Table 1).

Another overall mass transfer calculation approach is based on mass balance (18) applied to the feed tank. It is also assumed uniform mixing in the tank and acid concentration are always in excess to ensure the ammonia reaction.

$$-V \frac{d}{dt} C_{TAN,tank} = A K_{TAN} (C_{TAN,tank} - C^*_{TAN,feed}) \quad (18)$$

Where $C_{TAN,tank}$ is the concentration of ammonia in the tank, thus the inlet concentration of ammonia in the membrane contactor, $C^*_{TAN,feed}$ is equal to zero, as we explained before.

The integration and linearization of expression (18) allow to obtain the overall mass transfer coefficient K_{TAN} , equation (19):

$$\ln \left(\frac{C_{TAN,tank}(t)}{C_{TAN,tank}(t_0)} \right) = - \frac{A K_{TAN}}{V} \cdot t \quad (19)$$

This balance was reported in configurations 1, 2, 6, 9, 10 and 12 (Table 1).

There is no general agreement in using the two approaches; comparisons of mass transfer coefficients with other studies should be carefully made in function of the calculation method. Figure 3 shows the comparison between the calculation methods. In equation (19), $C_{TAN,feed}$ is considered constant along the membrane module instead of considering the decrease of this concentration with the transfer, as mass balance (10) described. Consequently, higher mass transfer coefficients are obtained with equation (19).

4.3. System c: Membrane contactor submerged in the feed solution

In the case of a system with the membrane fibres submerged in a tank (Figure 2c) containing the ammonia solution (configuration 4 or 9, Table 1), $C_{TAN,the feed}$ will be constant along the

membrane module if an ideal stirred-tank is assumed. In this case, equation (19) can be applied.

Several authors arranged mass balance (18) [38,30,43,44] to calculate the overall mass transfer by quantifying the transferred ammonia (m) from the feed tank.

$$dm = \frac{dC_{TAN, tank}(t)}{dt} \cdot V \quad (20)$$

Substituting $C_{TAN}(t)$ from the integration of mass balance (18):

$$C_{TAN,tank}(t) = C_{TAN,tank}(t_0) \cdot e^{\left(-\frac{A_M \cdot K_{TAN}}{V} \cdot t\right)} \quad (21)$$

Finally, the rearrangement and integration of expression (20) and (21) allows to obtain the mass transferred and thus K_{TAN} , expression (22). It has to be noted that this equation allows calculating the same mass transfer coefficient as equation (19).

$$M = C_{TAN,tank}(t_0) V \left(1 - e^{-\frac{K_{TAN} A_M}{V} \cdot t}\right) \quad (22)$$

For the same system but using a tubular membrane (configuration 9, Table 1), Samani Majd and Mukhtar, (2013b) used a less common approach. They first calculated ammonia fluxes (J_{NH_3}) based on the measured concentrations of $NH_{3(g)}$ captured in acid solution, $NH_{3(g)}$ was calculated from Anthonisen relation (fraction $N-NH_{3(aq)}$) and Henry's law ($N-NH_{3(g)}$). Then, they applied equation (8) to obtain K_{FAG} . Riaño et al., (2019) [45] calculated the overall mass transfer coefficient similar to Samani Majd and Mukhtar, (2013a) but with aqueous free ammonia concentration.

K_{TAN} is generally used in last expressions, but all mass balances can be calculated as a function of the different mass transfers coefficients described in section 4. Careful attention is

needed concerning mass transfer coefficient expressions, K_{FA} is often mistaken with K_{TAN} in the literature.

Figure 3 illustrates $C_{TAN, \text{ tank}(t)}$ or $C_{TAN, \text{ feed out}}$ using the explained calculation methods to compare systems a, b and c. As there is no feed recirculation in system a, the TAN concentration after one passage in the membrane contactor is illustrated for the same flow (Q) and feed volume (V) as systems b and c. In system c, if the ideal stirred-tank is assumed, the concentration gradient will be higher than the other systems (Equation (19), Figure 3).

If $C_{TAN, \text{ feed}}$ is considered constant along the membrane module, there will be no difference between the three mentioned systems (grey line, Figure 3). However, if the decrease of $C_{TAN, \text{ feed}}$ in the module is considered as equation (17) described, the mass transfer coefficient obtained will be lower in the case of system b (discontinuous line, Figure 3).

In Table 2, coefficients and equations are homogeneously summarized, independently of the nomenclature found in their corresponding article. All the mass transfer coefficients were obtained in studies at lab-scale except for two pilot-scale plants [45,57], and they were not remarkably higher than lab-scale coefficients. Further information concerning full-scale plants is needed to evaluate the effect of scale-up in mass transfer coefficients.

4.4. Modelling studies for predicting transfer coefficients of TMCS

Several models simulated the ammonia transport for membrane contactors operated with the feed stream flowing in shell side or lumen side (Table S.1). Mass transfer resistance of the acid side was considered negligible, independently if it was flowing in the shell or lumen side. Davey [3] confirmed this assumption experimentally by varying the concentration of the stripping solution from a $(NH_4^+)_2:SO_4^{2-}$ molar ratio of 0 to 1.5, the overall mass transfer

coefficient decreased significantly for the molar ratios higher to 1. However, no impact was found when acid was in excess.

When feed stream was flowing in shell side, mass transfer coefficient (k_s) can be estimated from empirical correlations based on the dependency of Reynolds (Re), Schmidt (Sc) and Sherwood (Sh) numbers. There is a multitude of empirical correlations for a hollow membrane contactor [56], but only ammonia removal studies were summarized in Table S.1. In a hollow-fibre contactor, membrane mass transfer coefficient (k_m) depends on membrane tortuosity, porosity, the fibre's wall thickness, and the diffusion coefficient of ammonia in the gas within the pores [3,5,25,28].

Different approaches were found concerning the mechanism of ammonia diffusion within the membrane's pores. It could be described as Knudsen diffusion [5,58] or a combination of Knudsen and bulk diffusion [58–60,31], depending on the size of the pores [61]. Hasanoğlu et al., (2010) [25] did not obtain any difference in transport description by using indistinctly Knudsen or bulk diffusion in their model. However, Reza kazemi et al., (2012) [58] compared a 2D mathematical model to the experimental results considering bulk diffusion and the combination of Knudsen and bulk diffusion. Knudsen was not predominant, but it slightly improved the accuracy of model predictions.

In a hollow-fibre contactor, when feed was flowing in lumen side under laminar flow conditions, mass transfer coefficient (k_l) was predicted via the well-known Leveque equation, which is based on the correlation between Sherwood and Reynolds, Schmidt, Gratz (Gz) numbers [28,62] or via Leveque expanded equation as a function of axial coordinate [5]. Gz number has to be higher than 6 to use these correlations [26].

Membrane and feed resistance will control the ammonia transfer. Nevertheless, calculating the theoretical coefficients is a complex task, and most authors prefer to measure the overall mass transfer coefficients from experimental systems.

Another approach of mass transfer 2D modelling is the resolution of conservation equations for feed side and membrane pores [60] considering molecular, and Knudsen diffusion, as well as the adsorption et desorption at the walls of the membrane pores during the transport through the membrane. The application of computational fluid dynamics (CFD) models was also studied [58,63].

5. Influencing parameters and optimal design

5.1. pH and temperature

The pH has a major role in TAN equilibrium, and it is one of the most critical factors determining TMCS performances [37]. Free ammonia fraction (FA) can be calculated using equation (23):

$$FA = \frac{1}{1 + 10^{(pK_a - pH)}} \quad (23)$$

where pK_a is the logarithmic dissociation constant (K_a) of ammonia calculated as equation (24) [64]:

$$K_a = 0.637 \cdot e^{\left(\frac{-6209}{T}\right)} \quad (24)$$

where T is the temperature in Kelvin.

Not only the ammonia-ammonium equilibrium is highly dependent on pH but also on temperature and ionic strength. At pH higher than 9, the temperature has a pronounced effect on $\text{NH}_3/\text{NH}_4^+$ ratio: the ammonia fraction increases from 0.06 at 0 °C to 0.74 at 50 °C (pH 9).

Several authors studied the influence of feed stream pH on the ammonia recovery and mass transfer coefficient (Table S.2). An increase on overall mass transfer coefficient K_{TAN} (Figure 4a) or ammonia removal was reported when pH increased from 8 to 10-11 [3,8,35,36,42,55,60], but it was not the case for pH values higher than 10 [8,31] or 11 [28,37]. This is logical when the transfer is defined on the total ammonia nitrogen, as the NH_3 concentration (for a given TAN) increases significantly in pH 8-11 but no longer for pH higher than 11. When the transfer is determined on the basis of K_{FA} (Figure 4b.), the coefficient should become theoretically independent of pH [41,42]. However, Figure 4b. illustrates that K_{FA} is a function of pH for values lower than 11 with an increasing [3,28] or decreasing [37,38,44] tendency. Therefore, using mass transfer coefficients to compare different TMCS performances for pH values lower than 11 is not appropriate if pH is not indicated in the study.

Increasing the temperature of the feed stream before entering into membrane contactor is beneficial for ammonia extraction. At least three explanations can be cited: the first is the modification of gas-liquid equilibrium (decrease of Henry's Constant), which promotes ammonia volatilization; secondly, the augmentation of diffusion coefficients of NH_3 at a higher temperature; thirdly, the modification of the acid-base equilibrium (ammonium/ammonia pKa decreases with increasing temperature) which promotes NH_3 fraction and hence the ammonia recovery.

The influence of temperature on ammonia removal was evaluated in several studies [25,42,48,55]. All authors confirmed an increase of ammonia removal with higher temperatures, between 20 °C and 40 °C. In addition, an apparent increase of K_{TAN} [38] coefficients was found with the increase of temperature. Concerning K_{FA} , it remained steady in the study of Wäeger-Baumann and Fuchs (2012) at pH 8.6, but it exponentially increased in the study of du Preez et al., (2005) [42] at pH >10 (Table S.2). This is logical because the temperature at low pH has a lower impact.

5.2. Effect of feed stream liquid velocity

The influence of feed velocity on the mass transfer coefficient was included in mentioned mass transfer correlations (Table S.1), as part of the Reynolds number. Mass transfer coefficient increases with the increase of velocity. This fact was experimentally observed in a hollow-fibre contactor [37,39] and can be explained by the reduction of the boundary layer close to the membrane surface with the increase of velocity [37]. However, it is also associated with a reduction of liquid retention time, decreasing the removal efficiency. At a full-scale plant, Ulbricht et al., (2013) [49] confirmed that the increase of flow rate increases the absolute NH_3 transferred but decreases the total ammonia removal efficiency. In contrast, the systems are operated with recirculation of the feed stream in most lab-scale studies, which can compensate this loss of efficiency.

From a modelling study, Mandowara and Bhattacharya (2011) predicted an increase in ammonia removal with the flow rate increase (configuration 2, Table 1). Nevertheless, it was observed that the impact on ammonia removal became negligible for a velocity higher than 0.15 m s^{-1} . In conclusion, increasing feed flow rate enhanced mass transfer in the given ranges, reducing the liquid resistance at the membrane-feed solution interface. However, the

mass transfer coefficient became independent of feed flow rate above a specific value. The mentioned studies about feed velocity impact are found in supplementary data (Table S.3).

5.3. Influence of initial ammonia concentration

Contradictory results about the effect of initial ammonia concentration on the removal efficiency and the mass transfer coefficient have been reported. Theoretically, the transfer rate is expected to be proportional to the initial concentration (eq. (6)-(8)), but the mass transfer coefficient should be independent of the initial concentration.

Several studies did not find any significant influence of the initial ammonia concentration on mass transfer coefficient [3,28,35,37,60] or ammonia removal [45,62].

However, more surprisingly, a decrease in the overall mass transfer coefficient was obtained when ammonia concentration increased [36,39,30,57]. This decrease of mass transfer coefficient with higher initial concentration was attributed to the increase of viscosity of concentrated solutions [28]. Although the independence of mass transfer coefficient from initial concentration was theoretically supported [59,62], further research is needed to clarify this impact. Indeed, the impact of increasing salinity with higher concentrations should also be considered. Table S.4 summarizes the primary information concerning cited studies.

5.4. Effect of salinity on feed solution

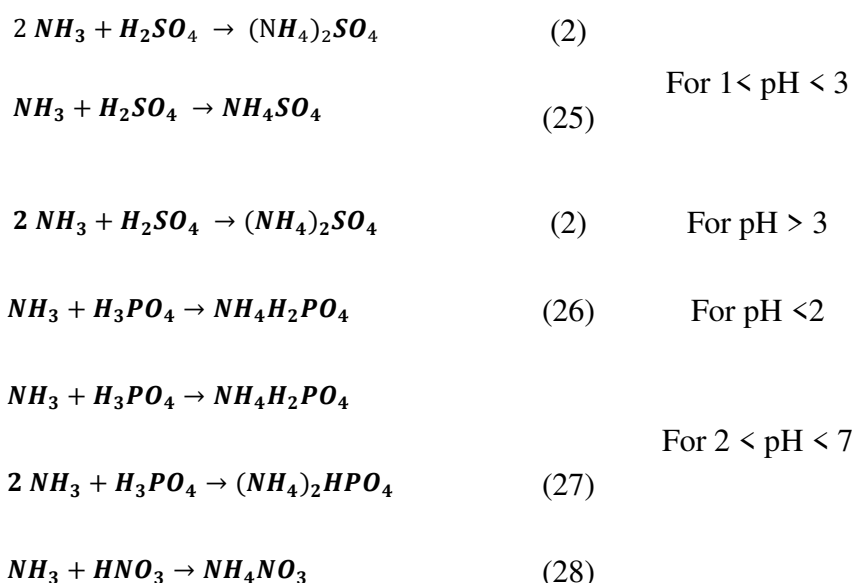
The influence of salinity in the feed stream has been poorly studied. Ashrafizadeh and Khorasani (2010) studied the effect of four salinity concentrations (0, 0.5 M, 1.0 M and 1.5M) on the overall mass transfer coefficient with a synthetic solution with an ammonia concentration of 800 mg L⁻¹. They did not find a significant effect on the mass transfer coefficient in the studied range of salt concentration.

The presence of ionic species in aqueous solutions can cause deviations from the “ideality” of the system due to intermolecular forces involved. To describe properly the equilibrium of a dissolved compound in presence of salts, activities should be used instead of concentrations.

5.5. Stripping solution: nature, concentration and liquid velocity.

On the acid side, conditions are usually chosen for maintaining a very low pH (< 2) through the membrane system to ensure an excess of protons reacting with free ammonia.

Diluted sulfuric acid is widely extended as a stripping solution; reported concentrations ranged from 0.001 M [55] to 1.3 M [5]. Nitric or phosphoric acids have drawn attention to producing fertilizer such as ammonium nitrate or ammonium phosphate. In function of the pH of the acid solution, different ammonia products could be obtained [65]:



Several authors have studied the impact of the stripping solution's nature, concentration, and liquid velocity on ammonia removal. A summary is available in Table S.5; pH values of the stripping solutions were calculated from the acid concentrations reported in each article.

Vecino et al., (2019) [24] compared two stripping solutions, HNO_3 , H_3PO_4 and a mixture of both acids. The highest ammonia removal was obtained with the stripping solution with a higher pH value corresponding to H_3PO_4 . Lai et al., (2013) [66] obtained higher removal from synthetic wastewater with the use of H_2SO_4 (pH 0.4) than with H_3PO_4 (pH 1.3) in a flat-sheet membrane; Damtie et al., (2021) [65] also found higher ammonia recovery with H_2SO_4 (pH 0.7) comparing to HNO_3 (pH 0.70), H_2PO_4 (pH 1.5) and a blend of these three acids. On the other hand, Nagy et al., (2019) [23] and Sancho et al., (2017) [22] did not find any significant difference using different acids, even if both solutions did not have the same pH value of the stripping solutions (Table S.5).

Hasanoğlu et al., (2010) [25] studied the effect of H_2SO_4 concentration (0.1 M - 0.3 M) and velocity on the recovery of ammonia for two different membrane contactors: flat-sheet and hollow-fibre. In the flat-sheet module, acid concentration did not seem to significantly influence the process for a high flow rate (99.9 L h^{-1}). However, at a lower flow rate (46.9 L h^{-1}) and highest acid concentration (0.3 M), ammonia removal slightly decrease, which could indicate an influence of acid concentration on the boundary layer when the flow rate is lower [25]. In the hollow-fibre module, when the flow rate was fixed at 120.0 L h^{-1} , they did not find an effect of acid concentration (0.1 – 0.3 M) on ammonia removal.

The impact of acid velocity and concentration on mass transfer coefficient was also studied [3,8,37]. Acid concentration did not significantly impact mass transfer or ammonia removal if the acid concentration was in excess. It could confirm that the reaction between ammonia and acid occurs at the interface of the acid stream in contact with the surface of the membrane [62].

However, Damtie et al., (2021) [65] found an optimal concentration of 0.01 M and 0.02 M for H_2SO_4 and H_3PO_4 , respectively, in the studied range of 0.005-0.6 M. The diluted

and concentrated solutions showed less ammonia captured. This could be linked to the fact that the pH quickly increased in the case of the diluted acid and the possible effect of viscosity in the case of concentrated points. In addition, the progressive increase in ammonium sulfate of the stripping solution did not show any impact on the mass transfer coefficient for $(\text{NH}_4)_2\text{SO}_4$ concentrations from 0 to 37 wt% [3].

To sum up, the velocity of the acid stream did not have a clear impact on ammonia removal, indicating that the resistance in the boundary layer of stripping solution is negligible in the studied acid velocities. Acid concentration is feed-specific; the concentration should be chosen to maintain an excess that ensures ammonia gradient across the membrane. The impact of the viscosity on ammonia removal in the case of higher acid concentrations needs further investigation. Furthermore, even if sulfuric acid is the most used one, contradictory results were found concerning the use of other acids. Comparisons were made on ammonia removal or mass transfer coefficient measurement. However, the impact of the nature of acid and concentration on vapour pressure and water transport was not evaluated, whereas the difference between feed and stripping solution is a driver of ammonia and water vapour transport (studied in 6.1).

6. Limiting factors

6.1. Water vapour transport

Undesired water vapour could diffuse through the membrane pores, negatively affecting the recovery process, diluting the acid stream and increasing the acid requirements. The reported influence of the temperature, feed flow rate, and type of stripping solution in water vapour transport [24,36,49,55] is summarized in Table S.6. Water transport can be measured experimentally by a mass balance in the acid solution and also taking into account the

ammonia transfer. If water vapour transport occurs, the volume of acid solution will increase [24,55].

Vecino et al., (2019) [24] reported that water vapour flux depends on the partial pressure difference between feed and stripping solution and the membrane permeability. Considering Raoult's law and non-ideality of the solution, where activities coefficients are different from zero, water vapour flux through the membrane (J_w , $L m^{-2} h^{-1}$) could be described by equation (29) [24]:

$$J_w = P_w (p_{w_f}^\circ \gamma_{w_f} x_{w_f} - p_{w_a}^\circ \gamma_{w_a} x_{w_a}) \quad (29)$$

Where P_w is the permeability of water vapour, p_w° the water vapour pressure, γ_w the water activity coefficient and x_w the water mole fraction. The feed stream is represented by "f" and the acid stream by "a".

They also quantified the water vapour flux experimentally by measuring the water transported from the feed tank to acid solution, in function of the type of acid used: H_3PO_4 , HNO_3 and a mixture of both. Lower water vapour transport was obtained when H_3PO_4 was used with $0.022 \pm 0.006 L m^{-2} h^{-1}$, equivalent to 0.11% of water vapour flow per feed flow ratio.

Ulbricht et al., (2013) [49] studied the influence of feed temperature and flow rate in water vapour transport. Feed flow rate did not affect the water transport significantly, but by varying feed temperature from 30 °C to 40 °C, they found an increase of water vapour transport from 119 $L h^{-1}$ to 150 $L h^{-1}$, representing a water to feed ratio of 0.79 and 1.00 %, respectively, while ammonia removal improved from 62% to 84%. From 40°C to 50°C, ammonia removal improved only by 5%, but water transport reached 205 $L h^{-1}$, water to feed ratio of 1.37%. Such a result cannot be generalised; it reveals that optimal temperature can be

chosen to find a compromise between that two phenomena. Concerning the ratio of acid added per kilogram of ammonia removed ($\text{L H}_2\text{SO}_4 \text{ Kg}^{-1}$ of NH_3): 1.27 at 30 °C. 1.21 at 40 °C and 1.70 at 50°C, the temperature of 40 °C was the optimal value concerning ammonia removal and acid dilution due to water vapour transport. The ratio of acid added per kilogram of ammonia removed, the water vapour flux and the water vapour flow per feed flow ratio were calculated from the data reported in the studies.

Ahn et al., (2011) [36] found that water vapour transport from feed to acid stream can be suppressed by heating stripping solution. They compared one experiment with both streams at the same temperature to another one with a difference of 13 °C. The ammonia removal rate was not significantly different in both experiments. Vapour pressure of acid stream increased and therefore pressure gradient is minimised to avoid water vapour transfer.

Fillingham et al., (2017) [55] quantified the water vapour transport with two different feeds. A value of $0.14 \text{ L h}^{-1}\text{m}^{-2}$ and $0.05 \text{ L h}^{-1}\text{m}^{-2}$ was obtained respectively with digestate and ammonium chloride solution.

The water vapour transfer phenomenon depends on the partial water pressure difference mainly influenced by the temperature and composition of the feed and acid solution.

6.2. Impact of suspended solids and fouling phenomenon

Little information is reported about the long-term loss of performances due to fouling, mainly because TMCS is a novel technology with a few recent full-scale applications.

In the short term, the impact of suspended solids on TMCS was evaluated at laboratory scale at different concentrations (Table S.7) with synthetic [36,67] and real wastewater [44]. A low negative [36,38,44] or a negligible [67] effect of suspended solids on

ammonia removal or mass transfer coefficient was reported. It was assumed that the increase in solids concentration increases viscosity, reducing diffusive transport to the membrane surface [40], but viscosity was not measured.

In the long term, the formation of a fouling layer during operation decreased the mass transfer [68] and origin wetting [7,68,32,69] that led to acid leakage into the feed stream in some studies [7,30,32]. A decrease in the contact angle of the membrane was generally found after continuous operation [7,54,68,69]. SEM-EDS, ICP-OES, and ATR-FTIR analyses [7,53,68,69] showed that fouling was formed mainly by proteins [69], lipids [68] or the presence of hydrocarbons, as dissolved methane, that can damage PP material, intermediately resistant to hydrocarbons [32]. PTFE generally showed better behaviour against fouling [53,54]. Cleaning techniques such as water, sodium hydroxide and citric acid solution, and a combination of two acid and alkaline commercial cleaning solutions were studied by Thygesen et al., (2014) [53]. Proteins were removed after all cleaning treatments in PTFE, but only after combining acid and alkaline commercial cleanings in PP. Carbohydrates were removed in PTFE only after the commercial solutions, but a percentage of lipids still remained. No technique could remove lipids and carbohydrates from PP.

Membrane biofouling was generally excluded considering the membrane hydrophobicity and the hard conditions of the process to allow biofilms to grow [53,69]. Concerning scaling, [68] reported the development of crystalline solids composed of CaCO_3 on the membrane surface when the pH of wastewater was 11, whereas it was not observed for pH 9.2.

Wetting, scaling, fouling or losing of membrane hydrophobicity in different membrane materials remind critical mechanisms to scrutinize TMCS process performances in the long term. In addition, wettability may also be responsible for the noticed water transport.

7. Practical feedbacks and future needs for a scale-up

About 40 studies in lab-scale, 8 at pilot scales, 3 at full scale were evaluated, indicating that the technology has reached a maturity level for which the scale-up methodologies are essential. While lab-scale studies evaluated synthetic solutions, bench and pilot plant studies treated anaerobic digester sludge liquor, manure, agro-food, urine, domestic wastewater or industrial effluents. Table S.8 summarizes the studies treating real wastewater and the range of ammonia concentration.

At full-scale, two plants were reported treating digestate [51,52] and another industrial wastewater [49]; all installations used PP hollow-fibre modules with the same system configuration (*Conf. 5*, Table 1). At pilot scale, three different configurations were found: submerged PTFE tubular membranes (*Conf. 9*, Table 1) to treat manure [70,71]; PP hollow-fibre membranes to treat the supernatant of digestate with the feed flowing on the shell side (*Conf. 5*, Table 1) [48] and a PP hollow-fibre membrane to treat permeate from the ultrafiltration of digestate flowing on lumen side (*Conf. 1*, Table 1) [42]. Table S.9 summarizes the cited studies' feed, strip solutions characteristics, and main TMCS performances. There is a general agreement concerning the temperature of the feed stream, ranging from 35 to 40 °C, because of the mentioned advantages in point 5.1. Furthermore, all these facilities have chosen H₂SO₄ as the stripping solution. However, the pH of the stripping solution ranged from <1.5 to 6 and the reported concentrations of (NH₄)₂SO₄ were very different. There is still a lack of optimisation of pH and initial acid concentration in the

stripping stream. Indeed, the produced ammonium salt concentration choice will be linked to fertilising products regulations and market placing.

The summarized streams treated by TMCS in Table S.8 contain high organic matter concentrations and suspended solids concentration, and alkalinity. Consequently, TMCS technology needs to be included in a global process chain including pretreatments to protect from suspended matters and foulants and increase the pH and temperature in the optimal range, representing a major technical and economic challenge. To protect the membrane from suspended solids in the full-scale TMCS facilities, the systems included a 10 μm pre-filtration [49], a combination of lamella settler, sand filter and 1 μm pre-filtration [4] and a lamella settler, depth filtration, disc filters (30 μm) and 1-3 μm pre-filtration [52].

Appropriate pretreatment to adjust the pH of the feed stream is a key point for both performance and economic aspects of the process. It was reported as the main cost in the full-scale plant at Yverdon-les-Bains WWTP [4,48]. Generally, two methods were applied: the addition of a base or/and CO_2 stripping with aeration. Manure or digestate usually have a high buffer capacity due to the high concentration of bicarbonates. Initial pH is generally about 7-8 for digestate [72], 6-7 for fresh manure [73,74] and about 9 for storage urine [75,76]. CO_2 stripping can significantly reduce or even eliminate the base consumption necessary to increase the pH. In a packed CO_2 stripping column treating anaerobic digester centrate from a WWTP, with an airflow ratio of 8-10 air liquid⁻¹, the NaOH consumption decreased from 5.5-6.5 to 3.5-4.0 $\text{L}_{\text{NaOH}(50\%)} \text{KgN}_{\text{removed}}^{-1}$ [47]. For continuous aeration in the feed tank (configuration 9, Table 1), the aeration rate of 7.2 and 14.4 vvh (volume of air per volume of liquid per hour) increased around one unit the pH of the supernatant of digested manure [47,77] and swine manure [45,67,71,78].

Base addition was generally applied to increase the pH. Boehler, 2018 [4] reported the consumption of 1.7 mole NaOH mole⁻¹ $\text{N}_{\text{recovered}}$ where 80 % was consumed during pretreatment, 12 % in dosage between modules and 8% was used to increase the pH of final fertilizer in order to reach adequate pH for agriculture application. Indeed after TMCS treatment, a slight decrease of feed pH was reported [28,38] as desorbed NH_3 from feed stream shifts TAN equilibrium (1) and decreased the pH. A base substance was fed between several membrane modules in series to maximize NH_3 fraction and ensure high ammonia removal in the second stage [48].

Active research was dedicated to analysing and modelling the phenomenon at a laboratory scale. However, clear recommendations and methods for designing pilots and full-scale installation are still missing.

Moreover, economic analysis of the process is needed to elucidate the best operating conditions and applications, including the study of the most suitable configuration of the process in function of the influent and treatment objectives. In addition, multi-objective optimization of feed pH, temperature and flow will be necessary to find the optimal nexus between energy and chemicals consumption. This review classified and scrutinised the different configurations and methods for transfer coefficient determination. Such information should be used for proper design and scale-up.

The cost of TMCS process, including pretreatments but not the profit from ammonium sulfate sales, is calculated from pilot-scale facilities as 3.01 € $\text{KgN}_{\text{recovered}}^{-1}$ treating rendering condensate wastewater [54], 4.43 € $\text{KgN}_{\text{recovered}}^{-1}$ treating liquid manure [79], 3.43€ m^{-3} treating leachate, 5.16 € m^{-3} treating WWTP reject and 2.38 € m^{-3} treating urine [57]. The first data concerning the economic cost from pilot-scale was obtained. However, the cost improvement related to scale-up were not considered. From a global point of view, there

is a lack of comparison of this novel and promising technology with the available technologies for ammonia recovery and treatment, especially concerning the carbon footprint and the economics of the process at full-scale. First LCA study comparing conventional manure management and novel TMCS process has been conducted by González-García et al., 2022 [80], showing that TMCS scenario reduced the impact on global warming by 14%.

Up to now, regarding the techniques itself, only one hollow-fibre contactor made of PP (Membrana GmbH-3M) has been implanted at full-scale applications. First feedback reported the necessity of depth filtration to remove particulate matter [52], maybe because of the insufficient space between hollow fibres in such contactors [4]. Few studies have evaluated the fouling and wettability of the hydrophobic membranes used in TMCS [7,69,81] and none at full-scale. Cleaning protocols to prevent fouling and protect the membrane were poorly studied. Long-term evaluation of cleaning, fouling and membrane wetting should be investigated to determine the techno-economic feasibility of the process.

The price of fertilizers produced from recovered nutrients could potentially counteract the costs of TMCS operating conditions and membrane modules. Sulfuric acid is widely extended, but phosphoric and nitric acid could also be stripping solutions. A market survey of different types of fertilizers and demanded concentrations seems necessary to evaluate the economics of the process.

Some recent studies revealed the potential of TMCS for urine or source-separated effluent [6,23,26]. Indeed, decentralized approaches and source separation of wastewater have been drawn the world's attention [82–84]. They allow to limit the dilution of the resources and reach an appropriate concentration to be treated or recovered in areas close to the origin of the waste. Several studies used life cycle assessment (LCA) to evaluate the advantages of urine source separation compared to conventional wastewater treatment [85–87], concluding

that nutrient and wastewater management combined with treatment costs, specific scenarios of source separation are very beneficial and more advantageous than conventional processes. In this context, TMCS was included in the LCA of Besson et al., 2021 [88] to compare urine source separation, blackwater and greywater separation and conventional centralized treatment scenarios, showing the potential of TMCS as nitrogen recovery technology to reduce N_2O emissions compared to conventional wastewater treatments and producing a chemical fertilizer substitute. No experimental or model studies were found regarding the application of TMCS in the anaerobic digestion of blackwater (urine and faeces) from source separation, neither in the co-digestion with domestic organic wastes. Nevertheless, TMCS could be applied to deal with ammonia load during anaerobic digestion or digestate treatment after dewatering.

TMCS is a promising technology to recover ammonia from a wide range of waste such as digestate, urine, manure, tertiary or industrial effluents and control ammonia inhibition during anaerobic digestion. This review has detailed the multiple configurations of membrane contactors and the theoretical models of the process. Main modelling studies and mass transfer correlations concerning ammonia recovery in membrane contactors were summarized. The calculation methods for mass transfer coefficients were clarified, and it gives the possibility to compare different studies.

There is still a lack of knowledge about the water vapour transport phenomenon or the impact of operational conditions and water properties such as salinity. Special attention was given to the operational parameters such as temperature, pH, velocity, feed concentration and acid solution concentration and their impact on the performances of the process. The optimal balance between the increase of temperature, ammonia removal, the basis and acid

consumption has to be established to maximize nitrogen recovery but limit undesired phenomenon like water transport.

Up to now, membrane fouling studies have been very limited. Further research is needed to evaluate the long-term performances of membrane contactors and the most appropriate cleaning techniques. Pretreatment of the influent represents the main cost of the process; efforts to optimize this step or improve the membrane resistance to wetting and fouling have to be done. Upgrading to full-scale applications still needs further environmental and economic assessment to position the technology in the different application fields and place the recovered fertilizer in a scalable market.

8. Acknowledgements

This work is part of the DESIGN project funded by French National Research Agency (ANR-17-CE22-0017) and OMIX project funded by French Environment and Energy Management Agency (ADEME) and French Occitanie region.

9. References

- [1] J.S. Guest, S.J. Skerlos, J.L. Barnard, M.B. Beck, G.T. Daigger, H. Hilger, S.J. Jackson, K. Karvazy, L. Kelly, L. Macpherson, J.R. Mihelcic, A. Pramanik, L. Raskin, M.C.M. Van Loosdrecht, D. Yeh, N.G. Love, A New Planning and Design Paradigm to Achieve Sustainable Resource Recovery from Wastewater, *Environ. Sci. Technol.* 43 (2009) 6126–6130. <https://doi.org/10.1021/es9010515>.
- [2] S. Matassa, D.J. Batstone, T. Hülsen, J. Schnoor, W. Verstraete, Can Direct Conversion of Used Nitrogen to New Feed and Protein Help Feed the World?, *Environ. Sci. Technol.* 49 (2015) 5247–5254. <https://doi.org/10.1021/es505432w>.
- [3] C.J. Davey, M. Hermassi, E. Allard, M. Amine, N. Sweet, T.S. Gaité, A. McLeod, E.J. McAdam, Integrating crystallisation into transmembrane chemical absorption: Process intensification for ammonia separation from anaerobic digestate, *J. Membr. Sci.* 611 (2020) 118236. <https://doi.org/10.1016/j.memsci.2020.118236>.

- [4] M.A. Boehler, – WP4 – Nitrogen Management in Side Stream. D 4.3: Operation and Optimization of Membrane Ammonia Stripping, EAWAG, 2018. <http://www.powerstep.eu/resources/deliverables>.
- [5] P.A. Aligwe, K.K. Sirkar, C.J. Canlas, Hollow fiber gas membrane-based removal and recovery of ammonia from water in three different scales and types of modules, *Sep. Purif. Technol.* 224 (2019) 580–590. <https://doi.org/10.1016/j.seppur.2019.04.074>.
- [6] S.K. Pradhan, A. Mikola, H. Heinonen-Tanski, R. Vahala, Recovery of nitrogen and phosphorus from human urine using membrane and precipitation process, *J. Environ. Manage.* 247 (2019) 596–602. <https://doi.org/10.1016/j.jenvman.2019.06.046>.
- [7] X. Shi, J. Zuo, M. Zhang, Y. Wang, H. Yu, B. Li, Enhanced biogas production and in situ ammonia recovery from food waste using a gas-membrane absorption anaerobic reactor, *Bioresour. Technol.* 292 (2019) 121864.
- [8] M.C.S. Amaral, N.C. Magalhães, W.G. Moravia, C.D. Ferreira, Ammonia recovery from landfill leachate using hydrophobic membrane contactors, *Water Sci. Technol. J. Int. Assoc. Water Pollut. Res.* 74 (2016) 2177–2184. <https://doi.org/10.2166/wst.2016.375>.
- [9] M.E.R. Christiaens, K.M. Udert, J.B.A. Arends, S. Huysman, L. Vanhaecke, E. McAdam, K. Rabaey, Membrane stripping enables effective electrochemical ammonia recovery from urine while retaining microorganisms and micropollutants, *Water Res.* 150 (2019) 349–357. <https://doi.org/10.1016/j.watres.2018.11.072>.
- [10] C.M. Mehta, W.O. Khunjar, V. Nguyen, S. Tait, D.J. Batstone, Technologies to Recover Nutrients from Waste Streams: A Critical Review, *Crit. Rev. Environ. Sci. Technol.* 45 (2015) 385–427. <https://doi.org/10.1080/10643389.2013.866621>.
- [11] T. Yan, Y. Ye, H. Ma, Y. Zhang, W. Guo, B. Du, Q. Wei, D. Wei, H.H. Ngo, A critical review on membrane hybrid system for nutrient recovery from wastewater, *Chem. Eng. J.* 348 (2018) 143–156. <https://doi.org/10.1016/j.cej.2018.04.166>.
- [12] M.K. Perera, J.D. Englehardt, A.C. Dvorak, Technologies for Recovering Nutrients from Wastewater: A Critical Review, *Environ. Eng. Sci.* 36 (2019) 511–529. <https://doi.org/10.1089/ees.2018.0436>.
- [13] C. Vaneckhaute, V. Lebuf, E. Michels, E. Belia, P.A. Vanrolleghem, F.M.G. Tack, E. Meers, Nutrient Recovery from Digestate: Systematic Technology Review and Product Classification, *Waste Biomass Valorization.* 8 (2017) 21–40. <https://doi.org/10.1007/s12649-016-9642-x>.
- [14] R. Harder, R. Wielemaker, T.A. Larsen, G. Zeeman, G. Öberg, Recycling nutrients contained in human excreta to agriculture: Pathways, processes, and products, *Crit. Rev. Environ. Sci. Technol.* 49 (2019) 695–743. <https://doi.org/10.1080/10643389.2018.1558889>.

- [15] T.M.P. Martin, F. Esculier, F. Levavasseur, S. Houot, Human urine-based fertilizers: A review, *Crit. Rev. Environ. Sci. Technol.* 0 (2020) 1–47. <https://doi.org/10.1080/10643389.2020.1838214>.
- [16] D. Hou, D. Jassby, R. Nerenberg, Z.J. Ren, Hydrophobic Gas Transfer Membranes for Wastewater Treatment and Resource Recovery, *Environ. Sci. Technol.* 53 (2019) 11618–11635. <https://doi.org/10.1021/acs.est.9b00902>.
- [17] C. Eskicioglu, G. Galvagno, C. Cimon, Approaches and processes for ammonia removal from side-streams of municipal effluent treatment plants, *Bioresour. Technol.* 268 (2018) 797–810. <https://doi.org/10.1016/j.biortech.2018.07.020>.
- [18] A. Zarebska, D. Romero Nieto, K.V. Christensen, L. Fjerbæk Søtoft, B. Norddahl, Ammonium Fertilizers Production from Manure: A Critical Review, *Crit. Rev. Environ. Sci. Technol.* 45 (2015) 1469–1521. <https://doi.org/10.1080/10643389.2014.955630>.
- [19] M. Xie, H.K. Shon, S.R. Gray, M. Elimelech, Membrane-based processes for wastewater nutrient recovery: Technology, challenges, and future direction, *Water Res.* 89 (2016) 210–221. <https://doi.org/10.1016/j.watres.2015.11.045>.
- [20] M. Darestani, V. Haigh, S.J. Couperthwaite, G.J. Millar, L.D. Nghiem, Hollow fibre membrane contactors for ammonia recovery: Current status and future developments, *J. Environ. Chem. Eng.* 5 (2017) 1349–1359.
- [21] P. Luis Alconero, *Fundamental Modeling of Membrane Systems*, 2018. <https://dial.uclouvain.be/pr/boreal/object/boreal:199238> (accessed March 22, 2022).
- [22] I. Sancho, E. Licon, C. Valderrama, N. de Arespachaga, S. Lopez-Palau, J.L. Cortina, Recovery of ammonia from domestic wastewater effluents as liquid fertilizers by integration of natural zeolites and hollow fibre membrane contactors, *Sci. Total Environ.* 584 (2017) 244–251. <https://doi.org/10.1016/j.scitotenv.2017.01.123>.
- [23] J. Nagy, J. Kaljunen, A.J. Toth, Nitrogen recovery from wastewater and human urine with hydrophobic gas separation membrane: experiments and modelling, *Chem. Pap.* 73 (2019) 1903–1915. <https://doi.org/10.1007/s11696-019-00740-x>.
- [24] X. Vecino, M. Reig, B. Bhushan, O. Gibert, C. Valderrama, J.L. Cortina, Liquid fertilizer production by ammonia recovery from treated ammonia-rich regenerated streams using liquid-liquid membrane contactors, *Chem. Eng. J.* 360 (2019) 890–899. <https://doi.org/10.1016/j.cej.2018.12.004>.
- [25] A. Hasanoğlu, J. Romero, B. Pérez, A. Plaza, Ammonia removal from wastewater streams through membrane contactors: Experimental and theoretical analysis of operation parameters and configuration, *Chem. Eng. J.* 160 (2010) 530–537. <https://doi.org/10.1016/j.cej.2010.03.064>.
- [26] J. Zhang, M. Xie, X. Tong, S. Liu, D. Qu, S. Xiao, Recovery of ammonium nitrogen from human urine by an open-loop hollow fiber membrane contactor, *Sep. Purif. Technol.* 239 (2020) 116579. <https://doi.org/10.1016/j.seppur.2020.116579>.

- [27] Y. Qin, J.M.S. Cabral, S. Wang, Hollow-fiber gas-membrane process for removal of NH₃ from solution of NH₃ and CO₂, *AIChE J.* 42 (1996) 1945–1956. <https://doi.org/10.1002/aic.690420715>.
- [28] Z. Zhu, Z. Hao, Z. Shen, J. Chen, Modified modeling of the effect of pH and viscosity on the mass transfer in hydrophobic hollow fiber membrane contactors, *J. Membr. Sci.* 250 (2005) 269–276. <https://doi.org/10.1016/j.memsci.2004.10.031>.
- [29] J. Lakner, G. Lakner, P. Bakonyi, K. Belafi-Bako, Kinetics of TransMembrane ChemiSorption for waste water with high ammonia contents, *Desalination Water Treat.* 192 (2020) 444–450. <https://doi.org/10.5004/dwt.2020.25872>.
- [30] B. Lauterböck, M. Ortner, R. Haider, W. Fuchs, Counteracting ammonia inhibition in anaerobic digestion by removal with a hollow fiber membrane contactor, *Water Res.* 46 (2012) 4861–4869. <https://doi.org/10.1016/j.watres.2012.05.022>.
- [31] E. Licon, M. Reig, P. Villanova, C. Valderrama, O. Gibert, J.L. Cortina, Ammonium removal by liquid–liquid membrane contactors in water purification process for hydrogen production, *Desalination Water Treat.* 56 (2015) 3607–3616. <https://doi.org/10.1080/19443994.2014.974216>.
- [32] A. Bayrakdar, R.Ö. Sürmeli, B. Çalli, Dry anaerobic digestion of chicken manure coupled with membrane separation of ammonia, *Bioresour. Technol.* 244 (2017) 816–823. <https://doi.org/10.1016/j.biortech.2017.08.047>.
- [33] W. Rongwong, S. Sairiam, A modeling study on the effects of pH and partial wetting on the removal of ammonia nitrogen from wastewater by membrane contactors, *J. Environ. Chem. Eng.* 8 (2020) 104240. <https://doi.org/10.1016/j.jece.2020.104240>.
- [34] M. Sheikh, M. Reig, X. Vecino, J. Lopez, M. Rezakazemi, C.A. Valderrama, J.L. Cortina, Liquid–Liquid membrane contactors incorporating surface skin asymmetric hollow fibres of poly(4-methyl-1-pentene) for ammonium recovery as liquid fertilisers, *Sep. Purif. Technol.* 283 (2022) 120212. <https://doi.org/10.1016/j.seppur.2021.120212>.
- [35] M.J. Semmens, D.M. Foster, E.L. Cussler, Ammonia removal from water using microporous hollow fibers, *J. Membr. Sci.* 51 (1990) 127–140. [https://doi.org/10.1016/S0376-7388\(00\)80897-2](https://doi.org/10.1016/S0376-7388(00)80897-2).
- [36] Y.T. Ahn, Y.H. Hwang, H.S. Shin, Application of PTFE membrane for ammonia removal in a membrane contactor, *Water Sci. Technol. J. Int. Assoc. Water Pollut. Res.* 63 (2011) 2944–2948.
- [37] S.N. Ashrafizadeh, Z. Khorasani, Ammonia removal from aqueous solutions using hollow-fiber membrane contactors, *Chem. Eng. J.* 162 (2010) 242–249. <https://doi.org/10.1016/j.cej.2010.05.036>.
- [38] F. Wäeger-Baumann, W. Fuchs, The application of membrane contactors for the removal of ammonium from anaerobic digester effluent, *Sep. Sci. Technol.* 47 (2012) 1436–1442.

- [39] S. Kartohardjono, Iwan Fermi, Y. Yuliusman, K. Elkardiana, A. Putra Sangaji, A. Maghfirwan Ramadhan, The Removal of Dissolved Ammonia from Wastewater through a Polypropylene Hollow Fiber Membrane Contactor, *Int. J. Technol.* 6 (2015) 1146. <https://doi.org/10.14716/ijtech.v6i7.1845>.
- [40] A. Zarebska, H. Karring, M.L. Christensen, M. Hjorth, K.V. Christensen, B. Norddahl, Ammonia Recovery from Pig Slurry Using a Membrane Contactor—Influence of Slurry Pretreatment, *Water. Air. Soil Pollut.* 228 (2017). <https://doi.org/10.1007/s11270-017-3332-6>.
- [41] M. Schneider, I.W. Marison, U. von Stockar, Principles of an efficient new method for the removal of ammonia from animal cell cultures using hydrophobic membranes, *Enzyme Microb. Technol.* 16 (1994) 957–963. [https://doi.org/10.1016/0141-0229\(94\)90004-3](https://doi.org/10.1016/0141-0229(94)90004-3).
- [42] J. du Preez, B. Norddahl, K. Christensen, The BIOREK® concept: a hybrid membrane bioreactor concept for very strong wastewater, *Desalination.* 183 (2005) 407–415. <https://doi.org/10.1016/j.desal.2005.03.042>.
- [43] B. Lauterböck, M. Nikolausz, Z. Lv, M. Baumgartner, G. Liebhard, W. Fuchs, Improvement of anaerobic digestion performance by continuous nitrogen removal with a membrane contactor treating a substrate rich in ammonia and sulfide, *Bioresour. Technol.* 158 (2014) 209–216. <https://doi.org/10.1016/j.biortech.2014.02.012>.
- [44] X. Wang, W. Gabauer, Z. Li, M. Ortner, W. Fuchs, Improving exploitation of chicken manure via two-stage anaerobic digestion with an intermediate membrane contactor to extract ammonia, *Bioresour. Technol.* 268 (2018) 811–814. <https://doi.org/10.1016/j.biortech.2018.08.027>.
- [45] B. Riaño, B. Molinuevo-Salces, M.B. Vanotti, M.C. García-González, Application of Gas-Permeable Membranes For-Semi-Continuous Ammonia Recovery from Swine Manure, *Environments.* 6 (2019) 32. <https://doi.org/10.3390/environments6030032>.
- [46] A.A. Samani Majd, S. Mukhtar, Ammonia Diffusion and Capture into a Tubular Gas-Permeable Membrane Using Diluted Acids, *Trans. ASABE.* (2013) 1943–1950. <https://doi.org/10.13031/trans.56.10218>.
- [47] M.B. Vanotti, P.J. Dube, A.A. Szogi, M.C. García-González, Recovery of ammonia and phosphate minerals from swine wastewater using gas-permeable membranes, *Water Res.* 112 (2017) 137–146. <https://doi.org/10.1016/j.watres.2017.01.045>.
- [48] M.A. Boehler, A. Heisele, A. Seyfried, M. Grömping, H. Siegrist, (NH₄)₂SO₄ recovery from liquid side streams, *Environ. Sci. Pollut. Res.* 22 (2015) 7295–7305. <https://doi.org/10.1007/s11356-014-3392-8>.
- [49] M. Ulbricht, J. Schneider, M. Stasiak, A. Sengupta, Ammonia Recovery from Industrial Wastewater by TransMembraneChemiSorption, *Chem. Ing. Tech.* 85 (2013) 1259–1262. <https://doi.org/10.1002/cite.201200237>.

- [50] M.J. Rothrock, A.A. Szögi, M.B. Vanotti, Recovery of ammonia from poultry litter using flat gas permeable membranes, *Waste Manag.* 33 (2013) 1531–1538. <https://doi.org/10.1016/j.wasman.2013.03.011>.
- [51] M. Pürro, F. Gindroz, Stripping membranaire de l'ammoniaque, *Aqua Gas.* (2018) 26–29.
- [52] L. Richter, M. Wichern, M. Grömping, U. Robecke, J. Haberkamp, Ammonium recovery from process water of digested sludge dewatering by membrane contactors, *Water Pract. Technol.* 15 (2020) 84–91. <https://doi.org/10.2166/wpt.2020.002>.
- [53] O. Thygesen, M.A.B. Hedegaard, A. Zarebska, C. Beleites, C. Krafft, Membrane fouling from ammonia recovery analyzed by ATR-FTIR imaging, *Vib. Spectrosc.* 72 (2014) 119–123. <https://doi.org/10.1016/j.vibspec.2014.03.004>.
- [54] B. Brennan, C. Briciu-Burghina, S. Hickey, T. Abadie, S.M. al Ma Awali, Y. Delaure, J. Durkan, L. Holland, B. Quilty, M. Tajparast, C. Pulit, L. Fitzsimons, K. Nolan, F. Regan, J. Lawler, Pilot Scale Study: First Demonstration of Hydrophobic Membranes for the Removal of Ammonia Molecules from Rendering Condensate Wastewater, *Int. J. Mol. Sci.* 21 (2020). <https://doi.org/10.3390/ijms21113914>.
- [55] M. Fillingham, A. VanderZaag, J. Singh, S. Burtt, A. Crolla, C. Kinsley, J.D. MacDonald, Characterizing the Performance of Gas-Permeable Membranes as an Ammonia Recovery Strategy from Anaerobically Digested Dairy Manure, *Membranes.* 7 (2017) 59. <https://doi.org/10.3390/membranes7040059>.
- [56] S. Shen, S.E. Kentish, G.W. Stevens, Shell-Side Mass-Transfer Performance in Hollow-Fiber Membrane Contactors, *Solvent Extr. Ion Exch.* 28 (2010) 817–844. <https://doi.org/10.1080/07366299.2010.515176>.
- [57] J. Uz Kurt Kaljunen, R.A. Al-Juboori, A. Mikola, I. Righetto, I. Konola, Newly developed membrane contactor-based N and P recovery process: Pilot-scale field experiments and cost analysis, *J. Clean. Prod.* 281 (2021) 125288. <https://doi.org/10.1016/j.jclepro.2020.125288>.
- [58] M. Rezakazemi, S. Shirazian, S.N. Ashrafizadeh, Simulation of ammonia removal from industrial wastewater streams by means of a hollow-fiber membrane contactor, *Desalination.* 285 (2012) 383–392. <https://doi.org/10.1016/j.desal.2011.10.030>.
- [59] A. Mandowara, P.K. Bhattacharya, Simulation studies of ammonia removal from water in a membrane contactor under liquid–liquid extraction mode, *J. Environ. Manage.* 92 (2011) 121–130. <https://doi.org/10.1016/j.jenvman.2010.08.015>.
- [60] G.K. Agrahari, S.K. Shukla, N. Verma, P.K. Bhattacharya, Model prediction and experimental studies on the removal of dissolved NH₃ from water applying hollow fiber membrane contactor, *J. Membr. Sci.* 390–391 (2012) 164–174. <https://doi.org/10.1016/j.memsci.2011.11.033>.

- [61] N. Nagaraj, G. Patil, B.R. Babu, U.H. Hebbar, K.S.M.S. Raghavarao, S. Nene, Mass transfer in osmotic membrane distillation, *J. Membr. Sci.* 268 (2006) 48–56. <https://doi.org/10.1016/j.memsci.2005.06.007>.
- [62] X. Tan, S.P. Tan, W.K. Teo, K. Li, Polyvinylidene fluoride (PVDF) hollow fibre membranes for ammonia removal from water, *J. Membr. Sci.* 271 (2006) 59–68. <https://doi.org/10.1016/j.memsci.2005.06.057>.
- [63] F. Nosratinia, M. Ghadiri, H. Ghahremani, Mathematical modeling and numerical simulation of ammonia removal from wastewaters using membrane contactors, *J. Ind. Eng. Chem.* 20 (2014) 2958–2963. <https://doi.org/10.1016/j.jiec.2013.10.065>.
- [64] M. Roustan, *Transferts gaz-liquide dans les procédés de traitement des eaux et des effluents gazeux*, Tec & doc, Paris; Londres; New York, 2003.
- [65] M.M. Damtie, F. Volpin, M. Yao, L.D. Tijing, R.H. Hailemariam, T. Bao, K.-D. Park, H.K. Shon, J.-S. Choi, Ammonia recovery from human urine as liquid fertilizers in hollow fiber membrane contactor: Effects of permeate chemistry, *Environ. Eng. Res.* 26 (2021). <https://doi.org/10.4491/eer.2019.523>.
- [66] C.-L. Lai, S. Chen, R.-M. Liou, Removing aqueous ammonia by membrane contactor process, *Desalination Water Treat.* 51 (2013) 5307–5310.
- [67] S. Daguerre-Martini, M.B. Vanotti, M. Rodriguez-Pastor, A. Rosal, R. Moral, Nitrogen recovery from wastewater using gas-permeable membranes: Impact of inorganic carbon content and natural organic matter, *Water Res.* 137 (2018) 201–210. <https://doi.org/10.1016/j.watres.2018.03.013>.
- [68] W. Lee, S. An, Y. Choi, Ammonia harvesting via membrane gas extraction at moderately alkaline pH: A step toward net-profitable nitrogen recovery from domestic wastewater, *Chem. Eng. J.* 405 (2021) 126662. <https://doi.org/10.1016/j.cej.2020.126662>.
- [69] A. Zarebska, D.R. Nieto, K.V. Christensen, B. Norddahl, Ammonia recovery from agricultural wastes by membrane distillation: Fouling characterization and mechanism, *Water Res.* 56 (2014) 1–10. <https://doi.org/10.1016/j.watres.2014.02.037>.
- [70] A.A. Samani Majd, S. Mukhtar, Ammonia Recovery Enhancement Using a Tubular Gas-Permeable Membrane System in Laboratory and Field-Scale Studies, *Trans. ASABE.* (2013) 1951–1958. <https://doi.org/10.13031/trans.56.10261>.
- [71] B. Molinuevo-Salces, B. Riaño, D. Hernández, M.B. Vanotti, M.C. García-González, Membrane-based Nitrogen Recovery from Livestock Wastewater: A Pilot Plant Study, (2019). www.iwarr2019.org.
- [72] N. Korres, P. O’Kiely, J.A.H. Benzie, J.S. West, *Bioenergy Production by Anaerobic Digestion: Using Agricultural Biomass and Organic Wastes*, Routledge, 2013.

- [73] S.G. Won, W.S. Cho, J.E. Lee, K.H. Park, C.S. Ra, Data Build-up for the Construction of Korean Specific Greenhouse Gas Emission Inventory in Livestock Categories, *Asian-Australas. J. Anim. Sci.* 27 (2014) 439–446. <https://doi.org/10.5713/ajas.2013.13401>.
- [74] J. Huang, Z. Yu, H. Gao, X. Yan, J. Chang, C. Wang, J. Hu, L. Zhang, Chemical structures and characteristics of animal manures and composts during composting and assessment of maturity indices, *PLoS ONE*. 12 (2017). <https://doi.org/10.1371/journal.pone.0178110>.
- [75] H. Kirchmann, S. Pettersson, Human urine - Chemical composition and fertilizer use efficiency, *Fertil. Res.* 40 (1994) 149–154. <https://doi.org/10.1007/BF00750100>.
- [76] J.A. O’Neal, T.H. Boyer, Phosphate recovery using hybrid anion exchange: applications to source-separated urine and combined wastewater streams, *Water Res.* 47 (2013) 5003–5017. <https://doi.org/10.1016/j.watres.2013.05.037>.
- [77] P.J. Dube, M.B. Vanotti, A.A. Szogi, M.C. García-González, Enhancing recovery of ammonia from swine manure anaerobic digester effluent using gas-permeable membrane technology, *Waste Manag.* 49 (2016) 372–377. <https://doi.org/10.1016/j.wasman.2015.12.011>.
- [78] M.C. García-González, M.B. Vanotti, A.A. Szogi, Recovery of ammonia from swine manure using gas-permeable membranes: Effect of aeration, *J. Environ. Manage.* 152 (2015) 19–26. <https://doi.org/10.1016/j.jenvman.2015.01.013>.
- [79] B. Molinuevo-Salces, B. Riaño, M.B. Vanotti, D. Hernández-González, M.C. García-González, Pilot-Scale Demonstration of Membrane-Based Nitrogen Recovery from Swine Manure, *Membranes*. 10 (2020) 270. <https://doi.org/10.3390/membranes10100270>.
- [80] I. González-García, B. Riaño, R.M. Cuéllar-Franca, B. Molinuevo-Salces, M.C. García-González, Environmental sustainability performance of a membrane-based technology for livestock wastewater treatment with nutrient recovery, *J. Environ. Chem. Eng.* 10 (2022) 107246. <https://doi.org/10.1016/j.jece.2022.107246>.
- [81] B. Lauterböck, K. Moder, T. Germ, W. Fuchs, Impact of characteristic membrane parameters on the transfer rate of ammonia in membrane contactor application, *Sep. Purif. Technol.* 116 (2013) 327–334. <https://doi.org/10.1016/j.seppur.2013.06.010>.
- [82] T.A. Larsen, K.M. Udert, J. Lienert, eds., *Source separation and decentralization for wastewater management*, IWA Publ, London, 2013.
- [83] C. Thibodeau, F. Monette, C. Bulle, M. Glaus, Comparison of black water source-separation and conventional sanitation systems using life cycle assessment, *J. Clean. Prod.* 67 (2014) 45–57. <https://doi.org/10.1016/j.jclepro.2013.12.012>.
- [84] S. Hoffmann, U. Feldmann, P.M. Bach, C. Binz, M. Farrelly, N. Frantzeskaki, H. Hiessl, J. Inauen, T.A. Larsen, J. Lienert, J. Londong, C. Lüthi, M. Maurer, C. Mitchell, E. Morgenroth, K.L. Nelson, L. Scholten, B. Truffer, K.M. Udert, *A Research Agenda for*

the Future of Urban Water Management: Exploring the Potential of Nongrid, Small-Grid, and Hybrid Solutions, *Environ. Sci. Technol.* 54 (2020) 5312–5322. <https://doi.org/10.1021/acs.est.9b05222>.

- [85] S.K.L. Ishii, T.H. Boyer, Life cycle comparison of centralized wastewater treatment and urine source separation with struvite precipitation: Focus on urine nutrient management, *Water Res.* 79 (2015) 88–103. <https://doi.org/10.1016/j.watres.2015.04.010>.
- [86] K.A. Landry, T.H. Boyer, Life cycle assessment and costing of urine source separation: Focus on nonsteroidal anti-inflammatory drug removal, *Water Res.* 105 (2016) 487–495. <https://doi.org/10.1016/j.watres.2016.09.024>.
- [87] E. Igos, M. Besson, T. Navarrete Gutiérrez, A.B. Bisinella de Faria, E. Benetto, L. Barna, A. Ahmadi, M. Spérandio, Assessment of environmental impacts and operational costs of the implementation of an innovative source-separated urine treatment, *Water Res.* 126 (2017) 50–59. <https://doi.org/10.1016/j.watres.2017.09.016>.
- [88] M. Besson, S. Berger, L. Tiruta-barna, E. Paul, M. Spérandio, Environmental assessment of urine, black and grey water separation for resource recovery in a new district compared to centralized wastewater resources recovery plant, *J. Clean. Prod.* 301 (2021) 126868. <https://doi.org/10.1016/j.jclepro.2021.126868>.
- [89] E.E. Licon Bernal, C. Maya, C. Valderrama, J.L. Cortina, Valorization of ammonia concentrates from treated urban wastewater using liquid–liquid membrane contactors, *Chem. Eng. J.* 302 (2016) 641–649. <https://doi.org/10.1016/j.cej.2016.05.094>.
- [90] M.C. García-González, M.B. Vanotti, A.A. Szogi, Recovery of ammonia from swine manure using gas-permeable membranes: Effect of aeration, *J. Environ. Manage.* 152 (2015) 19–26. <https://doi.org/10.1016/j.jenvman.2015.01.013>.
- [91] B. Molinuevo-Salces, B. Riaño, M.B. Vanotti, M.C. García-González, Gas-Permeable Membrane Technology Coupled With Anaerobic Digestion for Swine Manure Treatment, *Front. Sustain. Food Syst.* 2 (2018). <https://doi.org/10.3389/fsufs.2018.00025>.

10. Tables and figures

- 1 Table 1: Membrane configurations in the function of the type of module, feed/stripping solution placement; recirculation or not and type of flow:
 2 co-current or countercurrent.

n°	Contactor	Feed stream	Stripping stream	Recirculation		Flow	Reference
				Feed stream	Stripping stream		
1	Hollow-fibre	Lumen-side	Shell-side	Yes	Yes	Co-current	Semmens et al., 1990; du Preez et al., 2005; Zhu et al., 2005; Tan et al., 2006; Ashrafizadeh and Khorasani, 2010
2		Lumen-side	Shell-side	Yes	Yes	Counter-current	[8,22,24,60,89]
3		Lumen-side	Shell-side	No	No	Counter-current	Aligwe et al., 2019
4		Submerged fibres	Lumen-side	No	Yes	Only stripping stream flow	[30,38,43,32,44]
5		Shell-side	Lumen-side	No	Yes	Counter-current	[49,48,51,52,26,54]
6		Shell-side	Lumen-side	Yes	Yes	Counter-current	[25,3,65]
7		Shell-side	Lumen-side	Yes	No	Counter-current	Kartohardjono et al., 2015
8	Flat-sheet	-	-	Yes	Yes	Co-current	[2462,8]
9	Tubular membrane	Submerged fibres	Lumen-side	No	Yes	Only stripping stream flow	[70,46,90,77,47,55,67,91,6,45,7,71,79]
10		Lumen-side	Shell-side	Yes	Yes	Counter-current	[40]
11		Lumen-side	Shell-side	Yes	No	Counter-current	[36]
12		Shell-side	Lumen-side	No	Yes	Counter-current	[23,57]

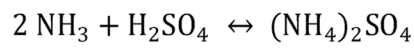
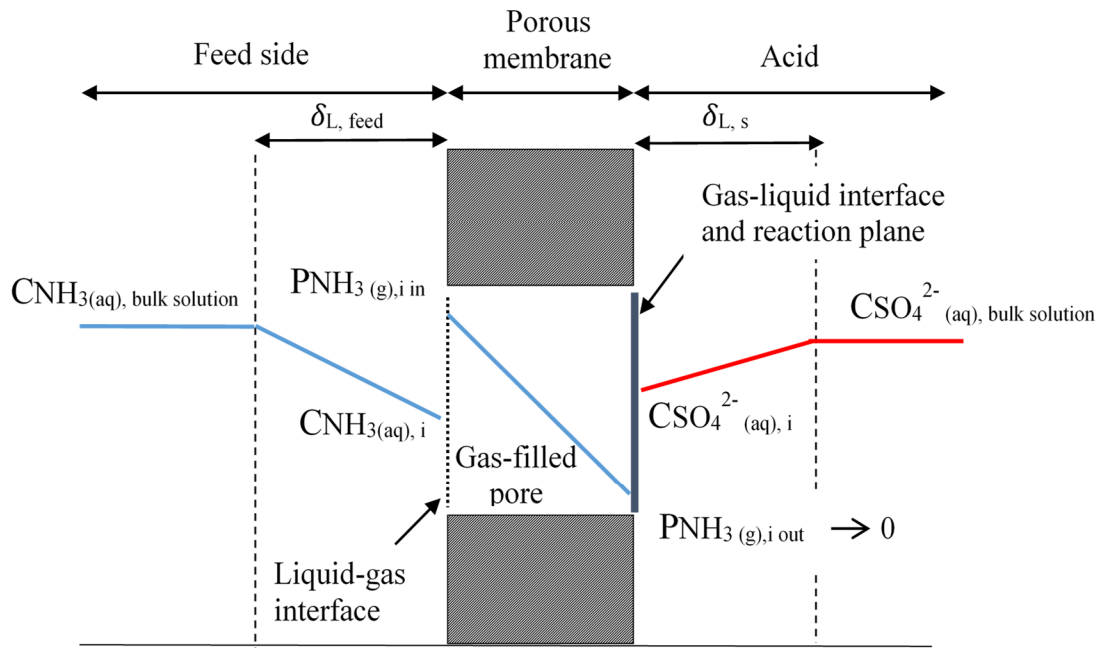
3 Table 2: Summary of overall mass transfer coefficients found in the literature from
 4 experimental studies. Configuration (Conf.) characteristics were described in Table 1.

Calculation	Eq.	Conf.	K (m s ⁻¹)	Reference
System a. (Figure 2): External membrane contactor without feed recirculation				
$K_{TAN} = \frac{Q}{A_M} \ln \left(\frac{C_{TAN(in)}}{C_{TAN(out)}} \right)$	(11)	3	1.7 · 10 ⁻⁶ ^{b)}	[5]
		5	2 · 10 ⁻⁷ – 6.0 · 10 ⁻⁷ ^{b)}	[26]
$\ln \left(\frac{C_{0(TAN)bulk\ feed}}{C_t(TAN)bulk\ feed} \right) = \frac{Q}{V} \left(1 - e^{-\frac{K_{TAN} a L}{v}} \right) \cdot t$	(17)	12	1.0 · 10 ⁻⁴ – 9.0 · 10 ⁻⁴ ^{b)}	[57]
$\ln \left(\frac{C_{TAN(t)}}{C_{TAN(t_0)}} \right) = -\frac{A K_{TAN}}{V} \cdot t$	(19)	12	2 · 10 ⁻⁷ – 5 · 10 ⁻⁷ ^{b)}	[57]
System b. (Figure 2): External membrane contactor with feed recirculation				
$\ln \left(\frac{C_{0(TAN)bulk\ feed}}{C_t(TAN)bulk\ feed} \right) = \frac{Q}{V} \left(1 - e^{-\frac{K_{TAN} a L}{v}} \right) \cdot t$	(17)	1; 11	2.0 · 10 ⁻⁶ ^{b)}	[35]
			4.3 · 10 ⁻⁶ – 3.8 · 10 ⁻⁵ ^{b)}	[36]
		7	2.0 · 10 ⁻⁴ – 4 · 10 ⁻⁵ ^{b)}	[39]
$\ln \left(\frac{C_{TAN(t)}}{C_{TAN(t_0)}} \right) = -\frac{A K_{TAN}}{V} \cdot t$	(19)	1	1.2 · 10 ⁻⁶ – 1.5 · 10 ⁻⁵	[37]
		10	4.7 · 10 ⁻⁶ – 8.1 · 10 ⁻⁶	[40]
		6	5.1 · 10 ⁻⁶	[3]
		1	1.1 · 10 ⁻⁵ – 1.3 · 10 ⁻⁵	[28]
		2	6.6 · 10 ⁻⁸ – 1.9 · 10 ⁻⁶	[24]
		2	0.2 – 0.5 · 10 ⁻⁵	[89]
		9	7.92 · 10 ⁻⁸	[7]
$\ln \left(\frac{C_{N-NH_3(t)}}{C_{N-NH_3(t_0)}} \right) = -\frac{A K_{FA} \cdot FA}{V} \cdot t$	(19)	1	4.3 · 10 ⁻⁶ – 3.8 · 10 ⁻⁵	[42]
System c. (Figure 2): Membrane contactor submerged in the feed solution				
$J_{NH_3} = K_{FAG} (C_{(N-NH_3(g))\ bulk\ feed} - C_{(N-NH_3(g))\ acid})$	-	9	1.0 · 10 ⁻⁶ – 9.2 · 10 ⁻⁶	[46]
$J_{TAN} = K_{FA} (C_{(N-NH_3(aq))\ bulk\ feed} - C_{(N-NH_3(aq))\ acid})$	-	9	1.5 · 10 ⁻⁵	[45]
$m = C_{TAN(t_0)} V \left(1 - e^{-\frac{K_{TAN} A_M t}{V}} \right)$	(21) ^{a)}	4	4.4 · 10 ⁻⁷ – 5.1 · 10 ⁻⁶	[38]
			2.5 · 10 ⁻⁷ – 1.5 · 10 ⁻⁶	[44]
$m = C_{N-NH_3(t_0)} V \left(1 - e^{-\frac{K_{FA} \cdot FA \cdot A_M t}{V}} \right)$	(21) ^{a)}	4	3.4 · 10 ⁻⁶ – 6.4 · 10 ⁻⁶	[38]
			2.8 · 10 ⁻⁶ ^{b)} 4.7 · 10 ⁻⁷ ^{b)} 6.9 · 10 ^{b)}	[30]
			8.7 · 10 ⁻⁷ ^{b)}	[43]
			1.0 · 10 ⁻⁶ – 1.4 · 10 ⁻⁵	[44]

5 a) Equation (21) is an arrangement of equation (19) but the formulation given by their
 6 authors was maintained in this table.

7 b) Approximated or averaged values from figures presented in the cited articles.

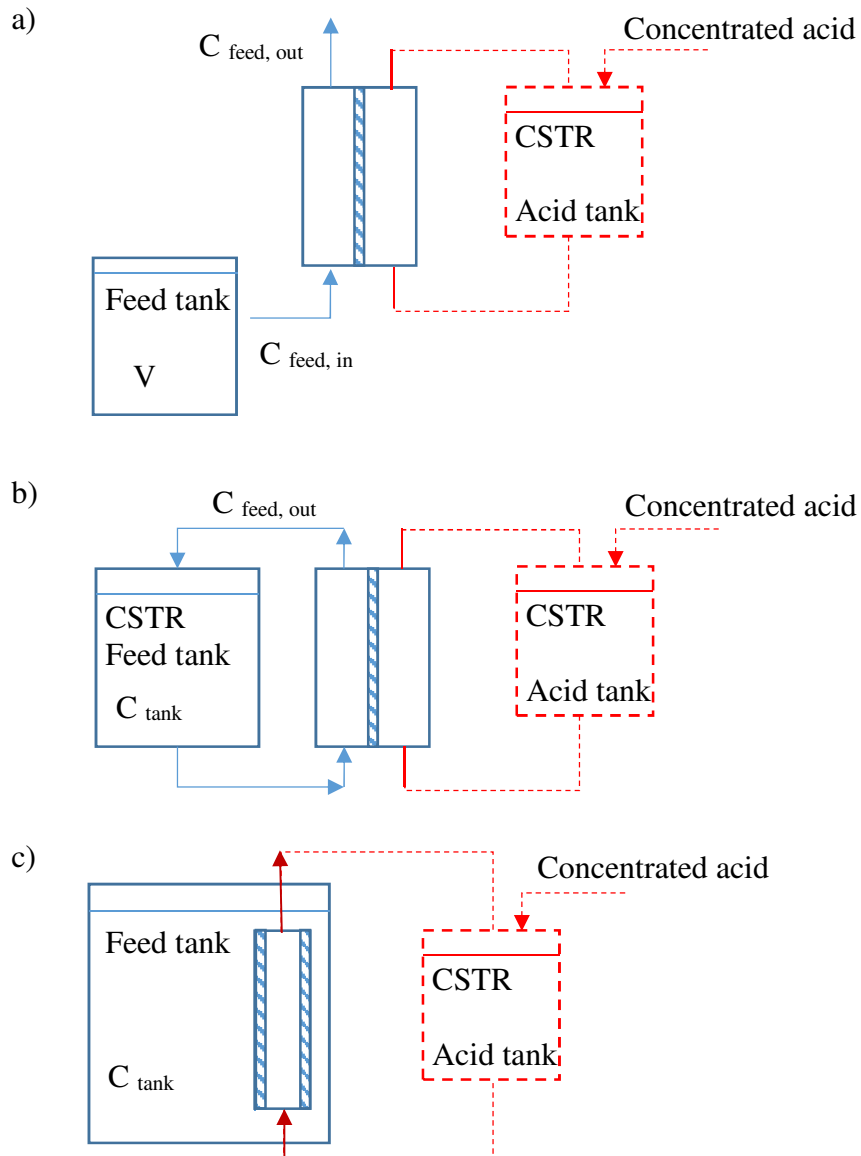
8



9

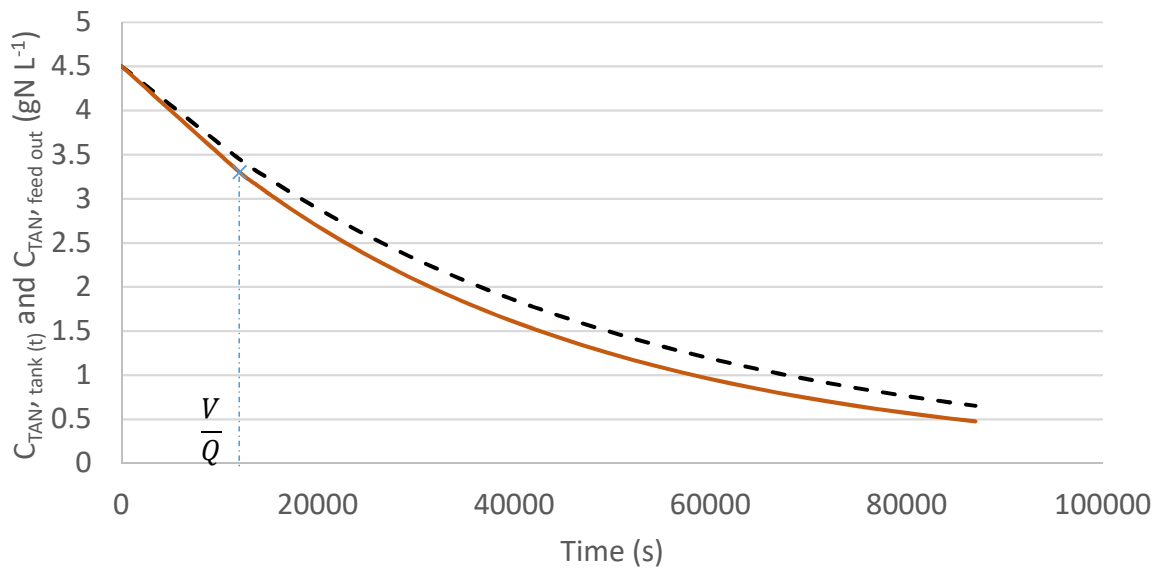
10 Figure 1: Concentration and partial pressure profiles for ammonia transport, “i” stands for the
 11 gas-liquid interface, “i in” and “i out” for the gas-liquid interface of pore entrance and exit,
 12 respectively. Mass transfer with an instantaneous reaction in the membrane surface and acid
 13 in excess is considered. Figure adapted from Hasanoğlu et al., (2010).

14



15 Figure 2: Schematic representation of the set-up: a. scheme of configurations 3, 5 and 12
 16 (Table 1) where feed and acid streams can flow in lumen or shell side and in a counter or co-
 17 current flow; b. scheme of configurations 1, 2, 6, 7, 10 and 11 (Table 1) where feed and acid
 18 streams can flow in lumen or shell side and in a counter or co-current flow of an external
 19 contactor; c. scheme of configurations 4 and 9 where the membrane contactor is directly
 20 submerged in the feed solution. The acid stream can be recirculated or not and concentrated
 21 acid can be added to ensure the acid excess conditions (dashed lines).

--- C TAN, tank(t) - System b (Equation 17) — C TAN, tan (t) - System b and c (Equation 19)
x C TAN, feed out - System a (Equation 11)



22

23 Figure 3: TAN concentration in the feed tank (system b and c) and the outlet of membrane
 24 module. Comparison of the approaches of mass transfer coefficient calculation: equation (11),
 25 equation (17) and equation (19). Parameters: $K_{TAN} = 1 \cdot 10^{-7} \text{ m s}^{-1}$, $A = 0.26 \text{ m}^2$, $L = 0.30 \text{ m}$, $Q =$
 26 $8.33 \cdot 10^{-8} \text{ m}^3 \text{ s}^{-1}$, $v = 9.02 \cdot 10^{-4} \text{ m s}^{-1}$, $V = 0.001 \text{ m}^3$, $a = 9302 \text{ m}^2 \text{ m}^3$

27

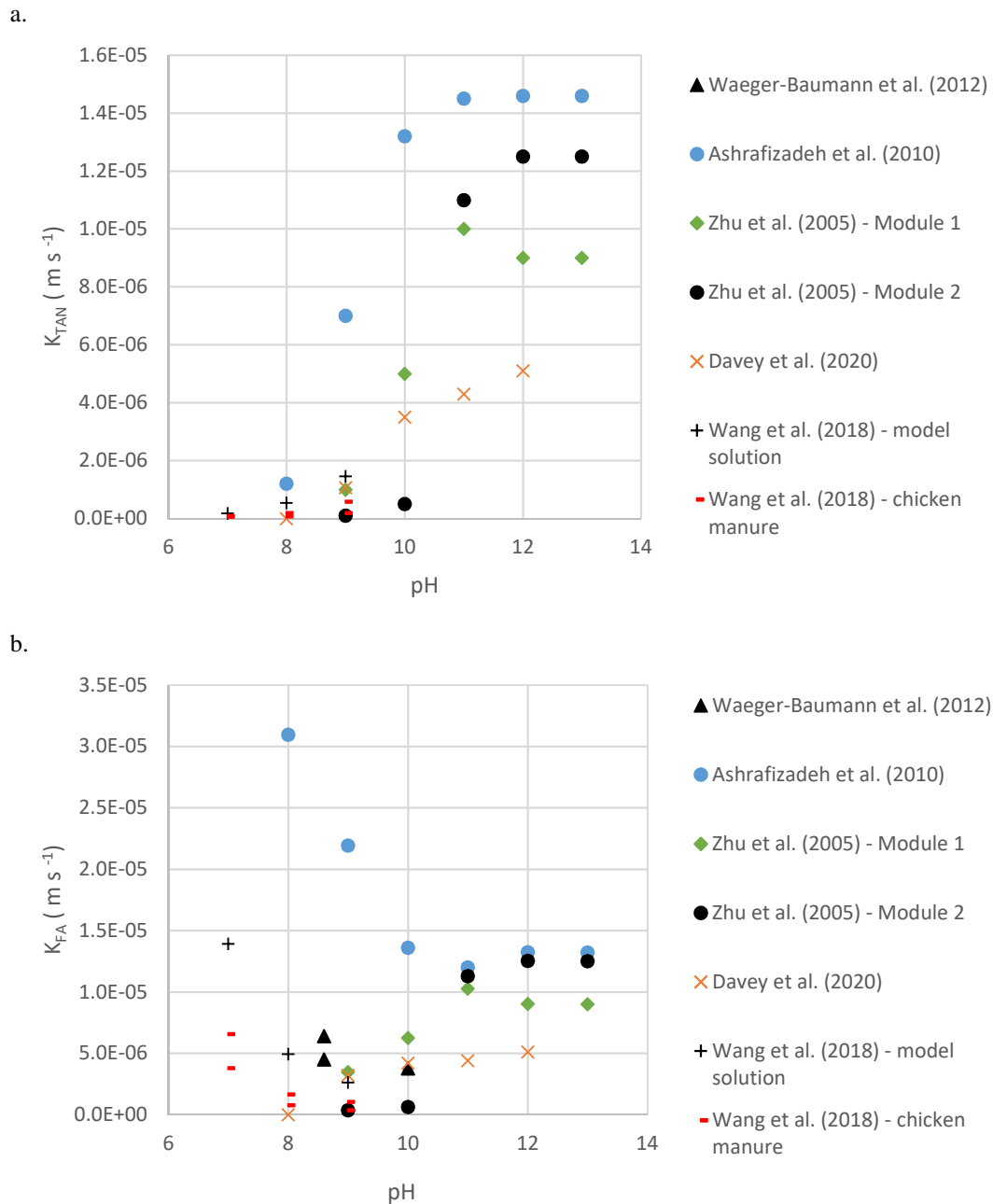


Figure 4: Ammonia mass transfer coefficient on the basis of total ammonia nitrogen K_{TAN} (a) and free ammonia K_{FA} (b) as a function of pH for several studies. If only K_{TAN} or K_{FA} was available in the studies, the other was recalculated from the existing coefficient, pH and temperature as $K_{TAN} = K_{FA} \cdot FA$, considering that pH and temperature did not change during operation.

System configurations

Mass transfer characterisation

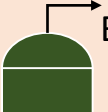
Operation conditions

Modelling and scale-up

NH₃ extraction. TMCS applications

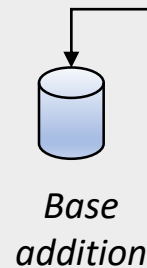
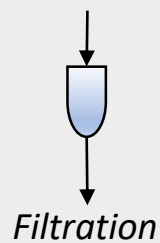
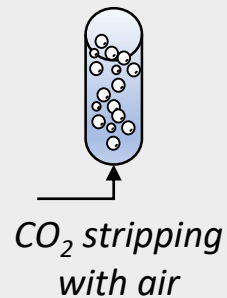
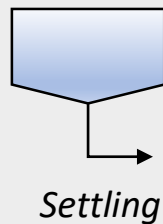

Manure and slurry


Urine


Biogas
Digestate


Wastewater

Pretreatment challenge



Transmembrane chemical absorption principle

